



Effect of Alumina Modification on the Reducibility of Co_3O_4 Crystallites Studied on Inverse-Model Catalysts

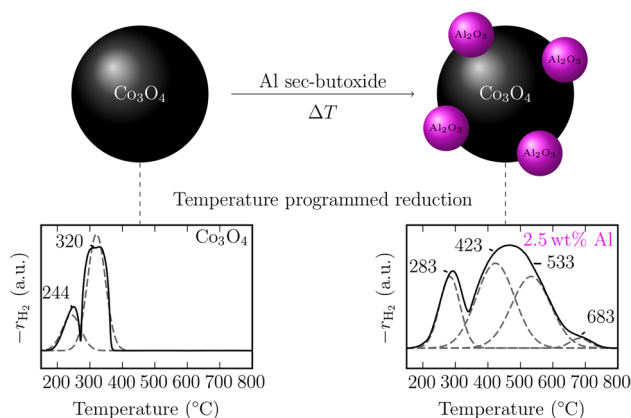
Anna P. Petersen¹ · Roy P. Forbes² · Sandeeran Govender¹ · Patricia J. Kooyman¹ · Eric van Steen¹

Received: 20 December 2017 / Accepted: 29 January 2018 / Published online: 22 February 2018
© Springer Science+Business Media, LLC, part of Springer Nature 2018

Abstract

In order to establish the effect of alumina modification and calcination temperature on the reducibility of cobalt oxide, alumina-modified cobalt oxide crystallites containing less than 2.5 wt% Al were prepared via incipient wetness impregnation, and calcined at 300 °C or 500 °C. The catalysts were characterised using X-ray diffraction, scanning transmission electron microscopy coupled with energy-dispersive X-ray spectroscopy, temperature programmed reduction (TPR) and X-ray absorption near edge spectroscopy. The alumina modification was found to prevent sintering during calcination and decrease the reducibility of the catalysts. With increasing alumina loading, and increasing calcination temperature, reduction peaks shift to higher temperatures and peaks above 400 °C appear in the TPR. The kinetic evaluation shows that the decreased reducibility is due to a decrease in the pre-exponential factor, which suggests that the alumina modification hinders hydrogen activation and the nucleation of reduced cobalt phases. The catalysts are completely reduced below 800 °C, and no CoAl_2O_4 phase formation was observed. TPR peaks between 400 and 650 °C were assigned to the formation of a non-stoichiometric cobalt–alumina phase with cobalt ions in octahedral coordination, while peaks between 650 and 800 °C correspond to cobalt ions in tetrahedral coordination. The results show that introduction of small amounts of alumina to cobalt oxide can have drastic effects on the rate of reduction and sintering.

Graphical Abstract



Keywords TPR · Metal-support interaction · Cobalt · Alumina

1 Introduction

The vast majority of industrial chemical processes involve the application of heterogeneous catalysts. In a typical heterogeneous catalyst, an active metal phase is dispersed on

✉ Eric van Steen
Eric.vansteen@uct.ac.za

Extended author information available on the last page of the article

an inert material, the catalyst support, in order to optimise catalytic activity. The main function of the catalyst support is to maintain a high dispersion of the catalytically active (metal) phase, but it also improves heat distribution and provides stability against abrasion. Such support materials are typically refractory oxides such as silica, alumina or titania, but also non-refractory materials such as carbon or silicon carbide can be used.

Despite the high chemical inertness of the materials used, the support may interact with the catalytically active phase and form mixed metal-support compounds. These mixed metal-support compounds may form during catalyst preparation or activation (reduction) [1, 2]. In the case of alumina-supported cobalt catalysts, the mixed metal-support compound cobalt aluminate (CoAl_2O_4) may be formed, which only reduces at temperatures above 800 °C. To minimise metal sintering, activation is typically performed at a temperature between 300 and 450 °C. Therefore, mixed-metal support compounds are termed ‘irreducible’ and are undesirable, since they lead to a loss in the availability of the catalytically active material. Hence, metal-support interactions have direct implications for the catalytic performance, which highlights the importance of understanding their formation.

The formation of metal-support interactions can be studied using temperature programmed reduction experiments. These can be used to investigate the effect of promoters [3–5], determine the presence of mixed-metal support compounds [6] and can even render kinetic information (e.g. activation energy) on the reduction process applying the Kissinger method [7].

The reduction of Co_3O_4 proceeds in two sequential steps: first to CoO and then to metallic cobalt [8]. Several authors have reported two peaks appearing around 250–300 °C and 300–400 °C for the reduction of bulk Co_3O_4 [3, 9–11]. The exact peak positions may vary depending on the experimental conditions (e.g. heating rate, reducing gas composition). The two main reduction peaks often overlap to a large extent [12] and are sometimes completely merged, resulting in only one visible peak [13–16]. Additionally, a peak appearing at temperatures below 250 °C is often reported, which is assigned to remaining cobalt precursor material that was not completely removed during calcination [17–20].

It should be noted that metal oxides supported on inert carriers, as is the case for a typical cobalt catalyst, may exhibit drastically different reduction patterns compared to bulk metal oxides [21]. Metal oxides may be homogeneously dispersed as small crystallites, in close contact with the support or as isolated islands of larger crystallites, in which case the reduction may be similar to that of the bulk oxide. For supported cobalt catalysts, the position and width of the second reduction peak are strongly dependent on the properties of the support [8]. Furthermore, the position of both reduction peaks shifts to lower temperatures with increasing

cobalt loading [12, 14] as well as with decreasing calcination temperature, suggesting that the peak position is related to the strength of the cobalt-support interaction [12, 22].

A broad reduction peak at temperatures above 400 °C and below 750–800 °C is generally assigned to cobalt-support interactions. Most authors seem to agree that a mixed cobalt-support phase is formed, which is limited to the support surface [16, 23]. Due to the difficulty of determining the structural changes occurring at the cobalt–alumina interface during reduction, the description of this phase is rather qualitative. It is often referred to as strongly or weakly interacting cobalt-support species, or cobalt surface support species, rather than describing a specific chemical composition [24].

A sharp reduction peak at temperatures above 750–800 °C can generally be assigned to stoichiometric CoAl_2O_4 . Cobalt aluminate, CoAl_2O_4 , may be formed during the temperature programmed reduction (TPR) experiment [6] but may also be present in calcined catalysts when the metal loading is very low (< 2 wt%), or the calcination temperature is above 750 °C [25].

The aim of this study is to gain fundamental insights into the effect of metal-support interactions on the reducibility of cobalt–alumina based catalysts. The concept is to use inverse model catalysts, in which the inert material is deposited onto the metal phase (similar to encapsulated catalysts) in contrast to conventional, supported catalysts, where the metal phase is deposited onto a porous inert material. This allows for a systematic study of metal-support interactions while excluding effects related to the physical properties of the support, such as porosity. The effect on the reducibility of cobalt oxide crystallites by introducing small amounts of alumina to their surface was studied using TPR, X-ray diffraction (XRD), scanning transmission electron microscopy coupled with energy-dispersive X-ray spectroscopy (STEM-EDS) and in-situ X-ray absorption near edge spectroscopy (XANES).

2 Experimental

2.1 Catalyst Preparation

Cobalt oxide with a crystallite size of 15–30 nm was prepared by calcination of a cobalt carbonate precursor. The resulting cobalt oxide crystallites are impregnated with aluminium sec-butoxide to render alumina-surface modified cobalt model catalysts. This method of preparation was necessary to prepare material in the desired crystallite size range. Cobalt carbonate was synthesised from a 0.5 M Co-containing solution prepared by adding 29.17 g $\text{Co}(\text{NO}_3)_2 \cdot 6\text{H}_2\text{O}$ to 200 ml demineralised water in a 1 l beaker. The pH of the solution was found to be between 5.6 and 5.8. Gaseous CO_2 was bubbled through a sparger

into the solution until the pH had reached 3.6. The solution was stirred, and 83.3 ml of a 0.25 M ammonia solution was added dropwise over the course of 10–15 min while bubbling CO₂ through the solution. A precipitate formed when the pH rose above 6. After ammonia had been added, the CO₂ flow was stopped, and the suspension was stirred for another 10 min before pressure filtration. Filtration leads to a slight increase in the pH of the filtrate, resulting in the formation of further precipitate. For that reason, the filtrate was collected and re-filtered three times. The combined precipitate was collected, and the filtrate was re-saturated with CO₂ until a steady pH was reached (pH 5.8–6). An additional 83.3 ml of a 0.25 M ammonia solution was added, and the suspension was stirred for 10 min before the filtration procedure was repeated. The filtrate was collected, and the procedure was repeated until a total of 500 ml ammonia solution had been added to the solution. This sequential precipitation and filtration procedure is necessary, as keeping the precipitate in the preparation mixture for extended periods, or adding ammonia quickly, may result in the formation of an (NH₄)₂Co₈(CO₃)₆(OH)₆ phase instead of the desired Co(CO₃)_{0.5}(OH)·0.11H₂O phase, which has a more favourable morphology. The combined precipitate was washed three times with 500 ml demineralised water. The precipitate was dried in air at room temperature for 48 h. After drying, the cobalt carbonate powder was ground and calcined in a static oven at 300 °C for 16 h. The resulting black Co₃O₄ powder was modified with alumina by impregnation with a dry solution of aluminium sec-butoxide in hexane, in an argon atmosphere, to achieve a weight loading of 0.1, 0.5 and 2.5 wt% Al, respectively, followed by calcination at 300 °C or 500 °C for 4 h. Pristine Co₃O₄ was also calcined at 300 and 500 °C to obtain unmodified reference samples. The catalysts are denoted 0.0Al300, 0.1Al300, 0.5Al300, 2.5Al300 and 0.0Al500, 0.1Al500, 0.5Al500, 2.5Al500 according to their aluminium weight loading and calcination temperature.

2.1.1 X-ray Diffraction (XRD)

X-ray diffraction (XRD) was performed on a Bruker AXS D8 advance diffractometer with Co-K α radiation ($\lambda = 1.78897 \text{ \AA}$) operating at 40 kV and 30 mA between 20° and 80° 2 θ with a scanning speed of 0.056° 2 θ /s. Line broadening of the Co₃O₄ (220) diffraction line was used to estimate the crystallite size using the Scherrer equation [26, 27].

2.1.2 Scanning Transmission Electron Microscopy-Energy-Dispersive X-ray Spectroscopy (STEM-EDS)

Scanning transmission electron microscopy-energy-dispersive X-ray spectroscopy (STEM-EDS) was performed using

a JEOL JEM-ARM200F double Cs-corrected TEM equipped with an FEG, a STEM unit and a high angle annular dark-field (HAADF) detector, operated at 200 kV. Samples were dispersed in methanol, ultra-sonicated for 2 min and transferred to a carbon coated copper grid. Samples on TEM grids were plasma cleaned for 45 s using a Gatan Solarus model 950 plasma cleaner at 25W under 20 ml/min Ar. EDX mapping was performed using an Oxford X-MaxN 100TLE detector and the Aztec software package.

2.1.3 Temperature Programmed Reduction (TPR)

Temperature programmed reduction (TPR) experiments were performed by weighing 45 mg sample into a quartz tube plugged with quartz wool and placed into a Micromeritics AutoChem HP-2950 TPR instrument. H₂ consumption was monitored with a thermal conductivity detector (TCD). The samples were dried at 120 °C for 1 h under 10 ml/min Ar and then cooled to 60 °C. Then the gas flow was switched to 5 vol% H₂ in Ar (flow rate 50 ml/min), and the samples were heated from 60 to 900 °C. Experiments were performed at a heating rate of 10, 5, 3 and 1 °C/min. The position of the peak maxima in the collected reduction profiles change as a function of heating rate according to the Kissinger equation [7]:

$$\ln \frac{\beta}{T_{max}^2} = -\ln \frac{E_a}{A \cdot R \cdot p_{H_2}^q} - \frac{E_a}{R} \cdot \frac{1}{T_{max}} \quad (1)$$

where β is the heating rate, T_{max} the temperature at peak maximum, E_a the activation energy, A the pre-exponential factor (or frequency factor), R the universal gas constant, p_{H_2} the hydrogen partial pressure and q the reaction order. The experiment was carried out under an excess of hydrogen. Thus, the reaction was assumed to be independent of the partial pressure of hydrogen. The activation energy and the pre-exponential factor can thus be determined from the slope and the intercept of the plot of $\ln \frac{\beta}{T_{max}^2}$ against $\frac{1}{T_{max}}$.

The rate constant (k) can then be determined using the Arrhenius equation

$$k = A \cdot e^{-\frac{E_a}{R \cdot T}} \quad (2)$$

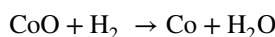
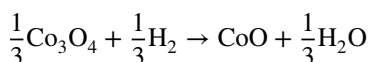
2.1.4 X-ray Absorption Near Edge Spectroscopy (XANES)

X-ray absorption near edge spectroscopy (XANES) experiments were carried out at the Brazilian Synchrotron Light Laboratory in Campinas, Brazil at the XAFS2 Beamline. The line uses a bending magnet (D08B@15_) and can be operated in an energy range of 4–17 keV. The beamline is equipped with a double crystal—Si(111) monochromator and has an energy resolution of $\Delta E/E = 1.71 \times 10^{-4}$ eV at 7 keV. A cylindrical mirror and a bendable and cooled

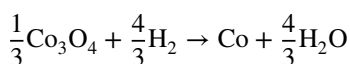
toroidal mirror are used as focusing elements to produce a beam size of $450 \times 250 \mu\text{m}^2$. All experiments were carried out in transmission mode at the cobalt K-edge of 7709 eV, and a Co metallic foil spectrum was collected simultaneously for energy calibration.

X-ray absorption near edge spectroscopy experiments were performed by collecting the background region from 7650 to 7700 eV in intervals of 2 eV, the XANES region from 7700 to 7800 eV was collected in intervals of 0.3 eV and the post-edge region from 7800 to 7900 eV at intervals of 2 eV for 1 s/step. For the in-situ experiments, 15 mg of sieved catalyst was diluted with 85 mg of boron nitride and then pressed into a disk. The disk was transferred onto a stainless-steel sample holder and placed in a tubular furnace. While collecting XANES, the catalyst was reduced in a flow of 50 ml{min of 5 vol% H_2 in He by heating to 150 °C at a heating rate of 10 °C/min and then further to 550 °C using a heating rate of 2 °C/min. Extraction of the XANES signal from the collected absorption spectra was carried out using the Demeter software package [28]. The background was removed using a second order polynomial for the pre-edge region and a third order polynomial for the post-edge region. The spectra were normalised by dividing by the height of the absorption edge. The phase composition during the reduction was determined via linear combination fitting in the region of -20 to 38 eV relative to the cobalt edge with the reference spectra.

For a better comparability of the results to the TPR experiments, a reduction profile (in terms of hydrogen consumption) can be calculated from the phase composition determined by the XANES experiments. The reduction of Co_3O_4 to CoO and metallic cobalt takes place in two sequential steps:



resulting in the overall stoichiometric equation:



The hydrogen consumption (X_{H_2}) and the rate of hydrogen consumption ($-r_{\text{H}_2}$) can then be calculated according to

$$X_{\text{H}_2} = \frac{1}{3} \cdot N_{\text{CoO}} + \frac{4}{3} \cdot N_{\text{Co}} \quad (3)$$

$$-r_{\text{H}_2} = \frac{dX_{\text{H}_2}}{dt} \quad (4)$$

where N_{CoO} and N_{Co} is the quantity of CoO and metallic cobalt, respectively, and t is the time. The rate of hydrogen

consumption corresponds to the reduction profile recorded during the TPR experiments.

3 Results and Discussion

Alumina-modified Co_3O_4 crystallites were prepared by impregnation of Co_3O_4 crystallites with varying amounts of alumina using aluminium sec-butoxide as the precursor. Co_3O_4 crystallites were obtained by calcination of a basic cobalt carbonate ($\text{Co}(\text{CO}_3)_{0.5}\text{OH}$) precursor at 300 °C. The XRD of the reference catalysts after drying and calcination is shown in Fig. 1.

The XRD of the dried precursor shows broad features indicating the compound was not well crystallised. The pattern corresponds to the crystalline phase of $\text{Co}(\text{CO}_3)_{0.5}(\text{OH}) \cdot 0.11\text{H}_2\text{O}$, which is in close agreement with the chemical formula of the synthesised compound determined by elemental analysis. After calcination at 300 °C, the material was oxidised to Co_3O_4 . The XRD shows broad diffraction lines indicating the formation of relatively small crystallites.

The XRD patterns of Co_3O_4 after modification with alumina shown in Fig. 2 show no additional diffraction lines, with the only detectable crystalline phase being that of Co_3O_4 . The alumina weight loading with a maximum of 2.5 wt% may be too low to be detectable by XRD. Furthermore, the alumina phase is expected to be very well dispersed on the surface of the catalyst, so that the alumina phase may not be crystalline enough to diffract the X-ray beam coherently. This was confirmed using high resolution TEM imaging and STEM-EDS mapping of the 2.5Al300 catalyst shown in Fig. 3. The EDS mapping shows that Al is homogeneously distributed as small clusters over the

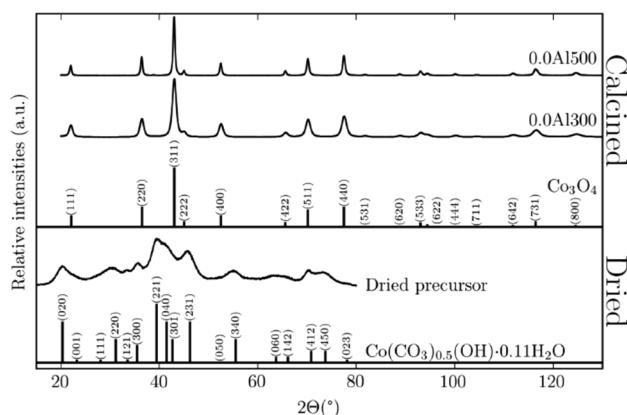


Fig. 1 X-ray diffraction of precipitated catalyst after drying and calcination. Dried precursor corresponds to crystalline phase of basic cobalt carbonate (PDF - 00-048-0083). Calcined catalysts correspond to crystalline phase of Co_3O_4 (PDF - 00-042-1467)

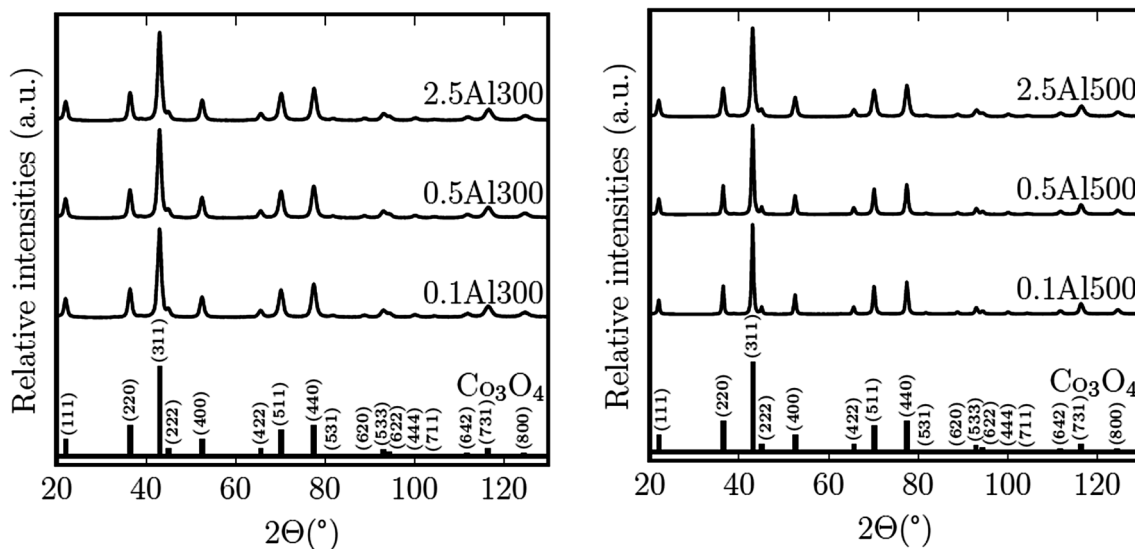


Fig. 2 X-ray diffraction of modified Co_3O_4 catalyst after calcination at 300 °C (left) and 500 °C (right) showing Co_3O_4 (PDF - 00-042-1467) as the only crystalline phase visible

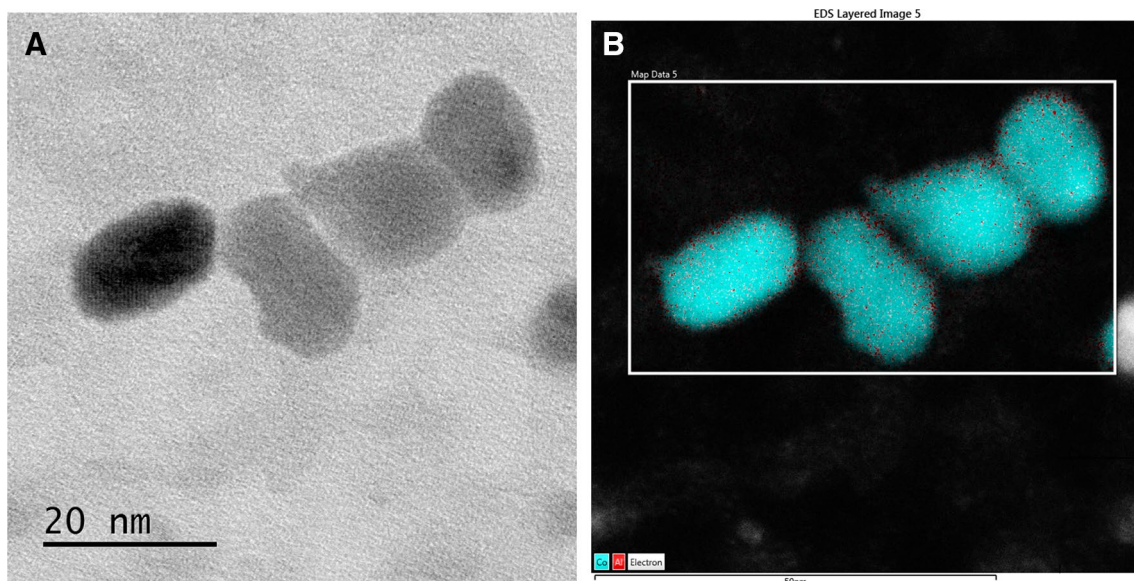


Fig. 3 Bright-field STEM and EDS mapping of 2.5Al300 showing Co in blue and Al in red. **a** 2.5Al300 bright field STEM. **b** Co and Al mapped using EDS

catalyst. The image shows a higher concentration of Al on the edges of the crystallites, indicating that the alumina phase is located at the Co_3O_4 surface.

Table 1 shows an overview of crystallite sizes determined for the different catalysts using XRD. The Co_3O_4 crystallite size of the catalysts calcined at 300 °C was 14 nm, independent of the alumina content. The crystallite size of the catalysts calcined at 500 °C was between 16 and 30 nm, and decreased with increasing alumina content. The catalysts were prepared by calcining cobalt carbonate at 300 °C

followed by impregnation and re-calcination of the catalyst at 300 °C or 500 °C. For the series of catalysts calcined at 300 °C, the temperature of the heat treatment before and after impregnation was the same. No crystallite growth was observed after impregnation, and the crystallite size was independent of the alumina content. However, when the calcination temperature after impregnation was increased to 500 °C, the crystallite size of Co_3O_4 increased with the crystallite size of Co_3O_4 in catalyst 0.0Al300 being 30 nm twice the size in the 0.0Al300 catalyst. However, the crystallite

Table 1 Cobalt oxide crystallite size and kinetic parameters of reduction for alumina-modified catalysts

T_{cal} (°C)	w_{Al} ^a (wt%)	$d_{\text{Co}_3\text{O}_4}$ ^b (nm)	Peak	E_a (kJ/mol)	A (s ⁻¹)	k^c (min ⁻¹)	$R^{2,d}$
300	0	14	1	126	4.1×10^{12}	38.0	0.96
			2	84	8.0×10^6	18.0	0.99
	0.1	14	1	146	5.8×10^{14}	41.3	0.76
			2	99	2.7×10^8	23.1	0.93
			3	53	2.3×10^3	8.2	0.97
	0.5	15	1	71	2.2×10^6	11.8	0.47
			2	70	3.0×10^5	14.1	0.79
			3	58	4.2×10^3	9.3	0.74
	2.5	14	1	67	5.9×10^5	17.0	0.92
			2	57	3.4×10^3	10.0	0.95
			3	66	2.8×10^3	9.0	0.92
			4	83	4.3×10^3	6.8	0.93
500	0	30	1	95	2.8×10^8	18.8	0.98
			2	69	1.4×10^5	13.2	0.99
	0.1	29	1	60	5.9×10^4	6.9	0.83
			2	54	4.2×10^3	6.4	0.92
			3	50	6.6×10^2	5.0	0.91
	0.5	25	1	73	1.4×10^6	16.3	0.95
			2	59	1.5×10^4	11.6	0.98
			3	60	5.7×10^3	9.8	0.99
			4	37	1.9×10^1	4.3	0.97
	2.5	16	1	61	$8.6 \cdot 10^4$	10.4	0.83
			2	54	1.5×10^3	7.6	0.91
			3	59	6.8×10^2	6.2	0.93
4			117	7.1×10^5	9.4	0.90	

^aAl weight loading calculated as g Al per g Co₃O₄

^bDetermined by XRD by FWHM of the (220) reflection using the Scherrer equation

^cRate constant k determined from the Arrhenius equation at the temperature of the peak maximum observed at a heating rate of 10 °C/min

^dCoefficient of determination for the linear regression analysis in the Kissinger plot

size of Co₃O₄ in catalyst 2.5Al500 was 16 nm, which is only slightly larger than in the catalysts calcined at 300 °C. This shows that small quantities of alumina can significantly reduce sintering during calcination.

The reducibility of catalysts was investigated using in situ XANES experiments (see Fig. 4) and TPR experiments (see Fig. 6). The in-situ XANES experiments were only performed on catalysts 0.0Al300, 0.5Al300 and 2.5Al300. The recorded spectra show that the white line intensity first increased as the catalysts were reduced to CoO and then decreased as they were further reduced to metallic cobalt. For the modified catalysts, a spike in the white line intensity corresponding to the formation of CoO is visible. This feature is less pronounced in the spectrum of the unmodified catalyst. The phase composition at each point was calculated by deconvolution of the scans with reference spectra collected for Co₃O₄, CoO and metallic cobalt (see Fig. 5). Formation of CoAl₂O₄ was not observed.

All catalysts show the sequential reduction of Co₃O₄ to CoO and then to metallic cobalt. CoO started to form around 100 °C, for unmodified Co₃O₄ and Co₃O₄ modified with 0.5 wt% Al, whereas CoO was only detected at around 200 °C when the Al content was 2.5 wt%. For all catalysts, metallic cobalt started to form around 300 °C. The rate of formation of metallic cobalt, however, decreased with increasing alumina content. At 550 °C the unmodified Co₃O₄ had been almost completely reduced to metallic cobalt, while the catalyst containing 2.5 wt% Al contained 14.5 wt% CoO.

In order to compare the in situ XANES and TPR experiments, the rate of hydrogen consumption during the XANES experiments was calculated, which corresponds to the reduction profiles determined during TPR experiments. When comparing the results of the XANES and the TPR experiments, the same trends can be seen. The reduction peaks shift to higher temperatures with increasing alumina

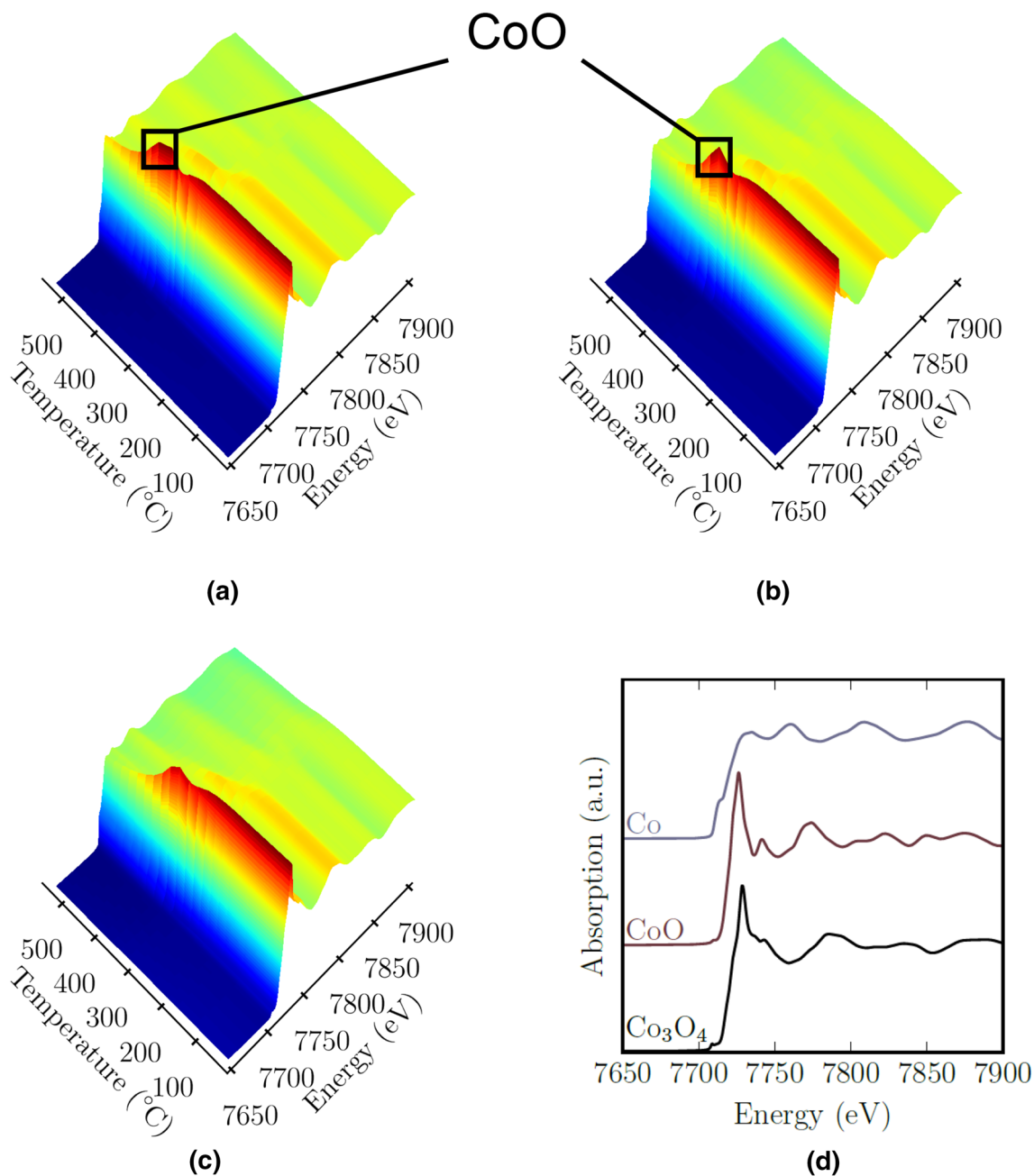


Fig. 4 XANES of unmodified and alumina-modified Co_3O_4 reduced in situ in H_2 . **a** 2.5Al300, **b** 0.5Al300, **c** 0.0Al300, and **d** reference spectra

loading and the reduction of unmodified Co_3O_4 shows only one broad peak.

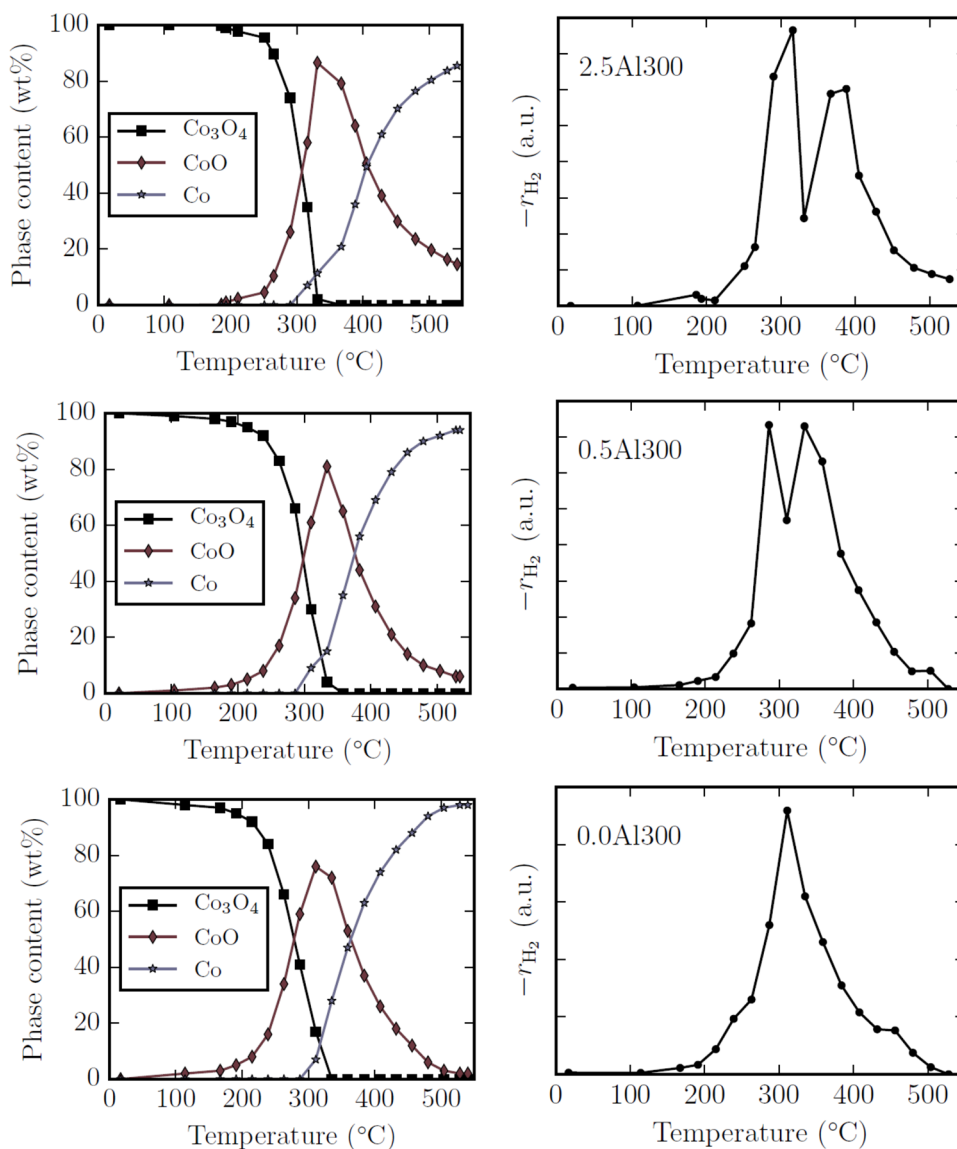
In order to study the kinetics of the reduction, TPR experiments were conducted at heating rates of 1, 3, 5 and 10 $^\circ\text{C}/\text{min}$. The shift of the peak maxima as a function of the heating rate can be used to calculate the kinetic parameters (E_a , A , k) of the underlying reduction process, by using the Kissinger equation [7]. The results are reported in Table 1.

The exact positions of the peak maxima were determined by peak deconvolution using a Gaussian function, because

of the large peak overlap visible in most of the experiments. The following section will focus on the results obtained at a heating rate of 10 $^\circ\text{C}/\text{min}$ for a better comparison with literature, as TPR experiments are routinely performed using this heating rate. The TPR profiles are shown in Fig. 6.

The reduction profiles of all catalysts show two main reduction peaks, corresponding to the formation of CoO and metallic cobalt, respectively. This is in line with the results obtained from the XANES analysis. For 0.0Al300, which is essentially bulk Co_3O_4 , these peaks have maxima

Fig. 5 Phase composition during reduction in H_2 of 2.5Al300, 0.5Al300 and 0.0Al300 (top to bottom) as calculated from linear combination fit of XANES spectra



at 250 and 329 °C. For 0.0Al500, the two reduction peaks strongly overlap, and the peaks shift to higher temperatures with maxima at 288 and 354 °C. This is consistent with the literature, where both one broad reduction peak and two reduction peaks have been reported for the reduction of bulk Co_3O_4 [6, 9–11, 13–16].

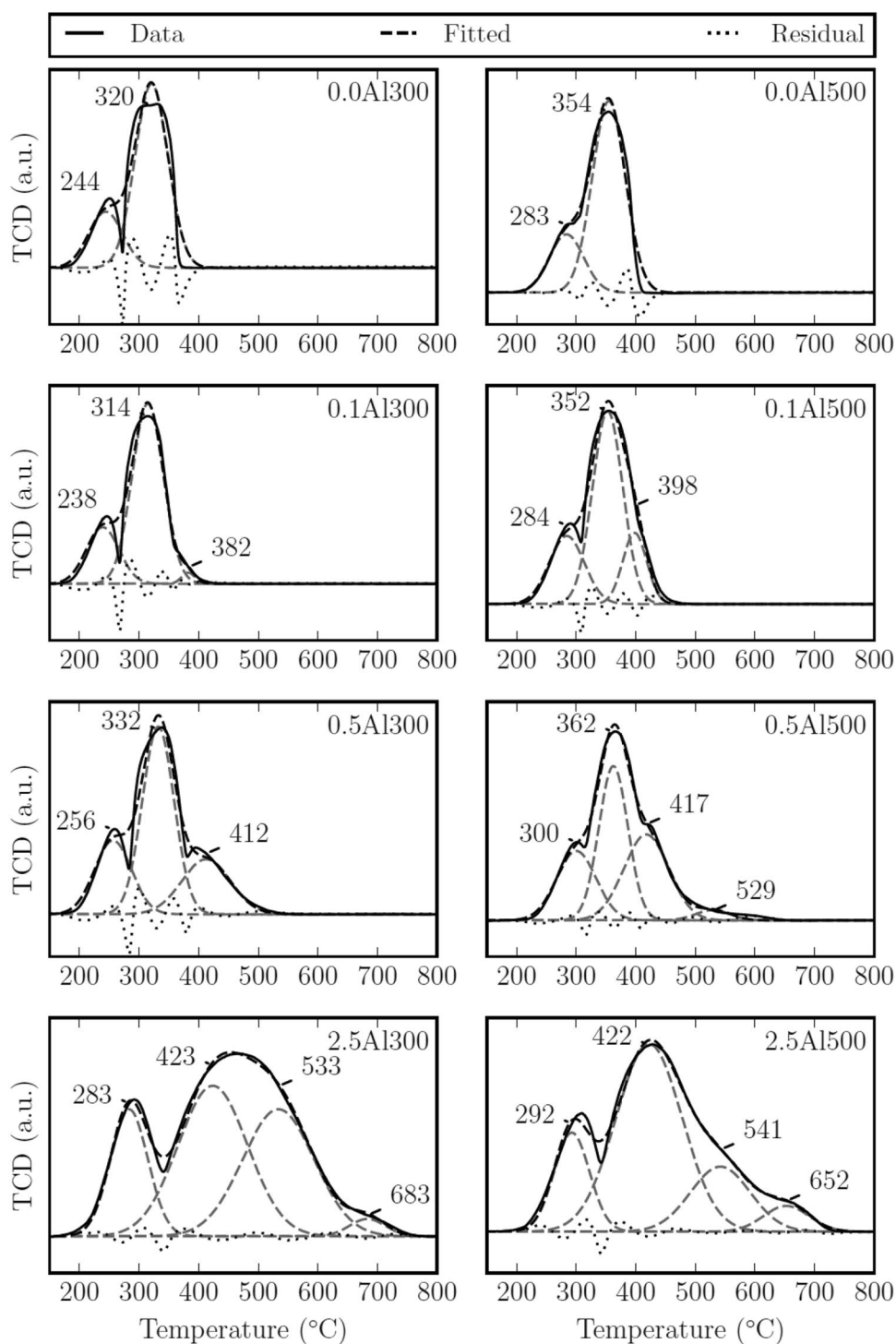
The activation energies calculated for the reduction of Co_3O_4 to CoO in the unmodified catalysts are 126 and 95 kJ/mol for the catalysts calcined at 300 and 500 °C, respectively. The activation energy calculated for the consecutive reduction of CoO to metallic cobalt is lower with 84 and 69 kJ/mol for calcination at 300 and 500 °C, respectively. Values reported in the literature vary widely, between 25 and 133 kJ/mol for the reduction of Co_3O_4 and 25–87 kJ/mol for the consecutive reduction of CoO [12, 29, 30]. This suggests that the activation energy, similarly to the reduction profiles, can vary widely with the method of Co_3O_4 preparation.

Despite the variations in the absolute value of the activation energy, the activation energies reported for the reduction of Co_3O_4 are consistently higher than those reported for the consecutive reduction of CoO to metallic cobalt.

In most studies, the reduction of bulk Co_3O_4 is merely reported for reference purposes, and little to no information is provided on the preparation or characterisation of the compound. However, it appears as though Co_3O_4 preparation involving harsh calcination conditions, such as temperatures above 400 °C and long calcination times, leads to a merging of the reduction steps resulting in a single peak in the reduction profile [14], while milder calcination conditions may result in a good resolution of the reduction steps [9], in agreement with the results obtained here.

The alumina-modified catalysts show significant peak broadening, a shift of the reduction peaks to higher temperatures, and additional peaks appearing above 400 °C. For

Fig. 6 Results of peak deconvolution for TPR experiments conducted at $10^\circ\text{C}/\text{min}$



catalysts containing 0.1 wt% Al and 0.5 wt% Al, a shoulder becomes visible with $T_{\text{max}} = 369\text{--}417^\circ\text{C}$, and for the catalysts with 2.5 wt% Al, the highest loading, a high temperature peak at $T_{\text{max}} = 647\text{--}685^\circ\text{C}$ can be observed. The first peak is shifted by $9\text{--}42^\circ\text{C}$ and the second peak is shifted by $9\text{--}139^\circ\text{C}$ compared to the unmodified catalyst. The peak shift increases with increasing alumina loading, except for

the 0.1Al300 catalyst, where the peaks are slightly shifted to lower temperatures, compared to the 0.0Al300 catalyst. It should be noted that the magnitude of the shift of the catalysts calcined at 500°C is smaller than for the catalysts calcined at 300°C , whereas the absolute value of T_{max} is larger. The catalysts are all completely reduced at temperatures below 800°C suggesting that CoAl_2O_4 was not formed,

in accordance with the results from the XANES experiments [6]. However, the shift in the peak temperature and the appearance of high temperature peaks are clear indicators for the presence of metal-support interactions [12, 21].

The shift of the reduction peaks to higher temperatures indicates a decrease in the rate of reduction. In fact, a decrease in the reaction constant (k) with increasing alumina content as well as with increasing calcination temperature was determined (except for catalyst 0.1Al300, which shall be discussed later). The decrease in the rate of reduction is correlated to a decrease in the pre-exponential factor (A). The pre-exponential factor decreased by at least one order of magnitude when alumina was introduced, and a clear trend was observed between the increase in alumina content and calcination temperature and a decrease in the pre-exponential factor. While the pre-exponential factor for the reduction of Co_3O_4 to CoO for the unmodified catalysts was $4.1 \times 10^{12} \text{ s}^{-1}$ and $2.8 \times 10^8 \text{ s}^{-1}$, the pre-exponential factor for catalysts modified with 2.5 wt% Al was much lower at $5.9 \times 10^5 \text{ s}^{-1}$ and $8.6 \times 10^4 \text{ s}^{-1}$, for calcination at 300 and 500 °C, respectively.

When alumina was introduced, the activation energies for both reduction steps decrease, except for catalyst 0.1Al300, whose activation energy is slightly higher at 146 kJ/mol compared to 126 kJ/mol for the 0.0Al300 catalyst. The activation energy is not directly related to the alumina content. Except for 0.1Al300, the activation energies for the reduction of the alumina-modified catalysts are of the same order of magnitude and vary between 60 and 73 kJ/mol for the reduction of Co_3O_4 to CoO , and between 54 and 70 kJ/mol for the reduction of CoO to metallic cobalt. Hence, the alumina modification in this study was found to affect the kinetics of the reduction of Co_3O_4 by decreasing the pre-exponential factor, and not the activation energy. Solid state reactions are often dominated by kinetic restrictions which may express themselves in the pre-exponential factor. This is because the rate of reduction of metal oxides is dominated by the rate of hydrogen activation and nucleation, which are correlated to the pre-exponential factor. In fact, it is a common misconception that the reducibility of an oxide is directly related to the metal-oxide bond strengths and thus the activation energy [31]. However, it should be noted that Ji et al. [12] made the opposite observation of metal-support interactions increasing the activation energy of the reduction.

The unmodified catalysts were completely reduced to metallic cobalt at about 380–400 °C, whereas the alumina-modified catalysts still contained considerable amounts of CoO , because of their decreased rate of reduction. At these temperatures, the ion mobility is large, and diffusion of Al-ions into the CoO matrix forming a non-stoichiometric cobalt alumina surface phase is possible. Co_3O_4 , CoO and CoAl_2O_4 all form crystal structures in which the oxygen

anions form an fcc lattice and the metal cations occupy a fraction of the octahedral and tetrahedral vacancies. Tetrahedrally coordinated Co^{2+} ions can be probed by XANES, showing a distinct, very intense pre-edge peak [32]. The in-situ XANES experiments showed no evidence for the presence of tetrahedrally coordinated Co^{2+} ions. It can be deduced that the Co^{2+} ions are octahedrally coordinated with the alumina phase. This is supported by Tsakoumis et al. [33], who investigated the reduction of a Re promoted $\text{Co}/\text{Al}_2\text{O}_3$ catalyst using in situ synchrotron XRD and reported a sudden expansion the $\gamma\text{-Al}_2\text{O}_3$ lattice parameter at the onset of CoO formation at 190 °C. This lattice expansion was explained by diffusion of Co^{2+} ions into octahedral vacancies in the $\gamma\text{-Al}_2\text{O}_3$ lattice forming a mixed cobalt-alumina phase.

It should be emphasised that the decrease in the reducibility of Co^{2+} ions in this mixed cobalt-alumina phase does not stem from a change in the cobalt-oxygen bond strengths. The results show that the activation energy of this phase is similar to the activation energy required for reduction of pure CoO . Instead, the pre-exponential factor is decreased. The Al ions in the cobalt–alumina matrix may simply decrease the rate of diffusion of cobalt ions thus hindering the nucleation of a metal phase. This phenomenon may be the origin of the third peak in the TPR-profile, appearing as a shoulder or broadening of the CoO peak in the reduction profile of alumina-modified cobalt catalysts.

This may be different for the catalysts containing 2.5 wt% Al. The high temperature peak appearing above 600 °C has a slightly higher activation energy of 83 and 117 kJ/mol, for calcination at 300 and 500 °C, respectively, and equal or higher pre-exponential factors than previous reduction steps. It should however be noted that the measured reduction temperature is too low for the reduction of stoichiometric CoAl_2O_4 . XANES experiments in this study were only conducted up to a temperature of 550 °C so that no information on the coordinative environment of the cobalt ions above 600 °C is available. Kurajica et al. [34] investigated the formation of sol–gel derived CoAl_2O_4 after annealing at different temperatures. They described the formation of an intermediate phase corresponding to Co_2AlO_4 at temperatures between 500 and 600 °C with Co^{3+} and a part of Co^{2+} ions in octahedral coordination. Annealing at 700 °C lead to formation of a CoAl_2O_4 spinel phase with a substantial degree of inversion (Co^{2+} ions in octahedral and tetrahedral coordination). According to Chin et al. [35], cobalt ions occupying tetrahedral sites in the alumina matrix (as in CoAl_2O_4) are more difficult to reduce than cobalt ions occupying octahedral positions. It may be assumed that the concentration of Al ions in the system was not high enough to allow the nucleation of a CoAl_2O_4 phase. It is hypothesised that at this point a non-stoichiometric cobalt-alumina phase

may be formed which may have Co^{2+} ions in tetrahedral coordination, which are more difficult to reduce.

Increasing the calcination temperature from 300 to 500 °C resulted in a decrease of the rate constant for reduction by about 20–40% when comparing catalysts with the same alumina content. These observations may be attributed to a change in crystallite size upon increasing the calcination temperature [36]. The crystallite size of Co_3O_4 calcined at 300 °C was 14 nm, which increased to 30 nm upon increasing the calcination temperature to 500 °C. An increase in crystallite size results in a decrease of surface area available for hydrogen dissociation which could lead to an increase of the induction period observed before the nucleation of a new phase [29, 37]. Figure 7 shows the degree of reduction (α) determined from TPR experiments as a function of time. The induction period for the reduction of 0.0Al300 was 15 min. This is about 5 min less than the induction time for 0.0Al500, corresponding to a difference in reduction temperature of about 50 °C. As a result, the estimated rate constant for Co_3O_4 reduction (k) at peak maximum decreased from 38 min^{-1} for 0.0Al300 to 19 min^{-1} for 0.0Al500.

The reduction curves for the 0.0Al300 catalyst show an S-curve for the first reduction step, corresponding to the formation of CoO, visible in the time range of 15–30 min. The S-shape is characteristic of a nucleation type process [38]. This suggests that hydrogen dissociation is slow, leading to a long induction period and slow nucleation. The freshly formed CoO nuclei grow until they form a layer around the unreduced Co_3O_4 core. At that point, the reduction slows down, due to mass transport limitations through the CoO shell. The shell thickness increases with increasing size

of the original Co_3O_4 crystallite. This will increase mass transport limitations by increasing the diffusion layer, and the reaction rate slows down. It can be concluded that the nucleation of the cobalt metal phase may occur before the Co_3O_4 core is completely reduced to CoO. This results in the strong overlap of the reduction processes and the merging of the reduction peaks visible in the TPR. This may also be a contributing factor to the observation that supported cobalt catalysts, which generally contain small Co_3O_4 crystallites, unlike bulk Co_3O_4 , typically show two well-resolved reduction peaks in the TPR.

Interestingly, the alumina modification seems to have the same effect on the induction period as increasing the calcination temperature. The onset of the formation of CoO, for both catalysts 2.5Al300 and 2.5Al500, was at about 20 min, similar to that of 0.0Al500, and larger than that of 0.0Al300. The crystallite size of 0.0Al300, 2.5Al300 and 2.5Al500 are practically identical (14 and 16 nm). Nonetheless, the surface area of Co_3O_4 crystallites might be partly reduced due to the alumina surface modification, which could explain the increased induction period. Moreover, the Al ions on the surface of the Co_3O_4 crystallites are not just expected to reduce the exposed Co_3O_4 surface but also occupy low energy sites, such as defect or step sites. Surface defects minimise the activation energy necessary for nucleation and are therefore good nucleation sites [39]. Ward et al. [40] imaged the reduction of Co_3O_4 to CoO using HRTEM, which showed that formation of CoO regions started on step sites and corners of the Co_3O_4 crystallites.

It should however be noted, that the effect of impurities (such as alumina deposited on the surface) on the number of defects and their effect on reaction kinetics is complex and may be specific to the type of reaction investigated and the quantity and type of impurity [41]. In some cases, an impurity may introduce lattice defects and increase the rate of reaction. This may explain the slight acceleration of the reduction observed for the 0.1Al300 catalyst. The very small quantity of Al present in this catalyst may have introduced, rather than blocked defect sites. This suggests that the effect may be strongly dependent on the concentration of the additive. This observation is also commonly made when studying the effect of chemical promoters in catalysts. Small promoter concentrations often positively affect the catalytic performance, while higher concentrations may reverse the effect resulting in an element-specific optimal promoter/Co-ratio [42].

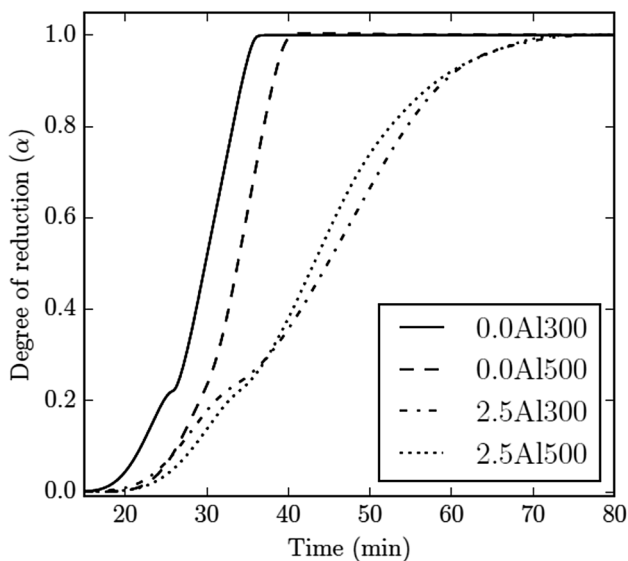


Fig. 7 Extent of reaction calculated from TPR of unmodified Co_3O_4 and modified with 2.5 wt% Al measured at a heating rate of 10 °C/min

4 Conclusion

In order to establish the effect of alumina modification and calcination temperature on the reducibility of cobalt oxide, alumina-modified cobalt oxide catalysts containing

less than 2.5 wt% Al were prepared by incipient wetness impregnation of cobalt oxide with aluminium sec-butoxide, followed by calcination at 300 or 500 °C. Alumina modification did not affect the structure of bulk Co_3O_4 , but stabilised small cobalt oxide crystallites, preventing metal sintering. The reducibility of the catalysts decreased with increasing calcination temperature and increasing alumina content.

The decrease in reducibility with increasing calcination temperature was attributed to an increase in the Co_3O_4 crystallite size. It should be noted that this effect is opposite to a common observation in supported catalysts, where reducibility decreases with decreasing the cobalt oxide crystallite size. This is because in supported catalysts the reducibility is dominated by metal-support interactions, which increases with decreasing crystallite size, due to a larger contact area of the metal oxide crystallite with the support. This emphasises the difference in the reduction behaviour of bulk and supported cobalt oxide. Astonishingly, the reduction profile of Co_3O_4 containing small amounts of 2.5 wt% Al has a stronger resemblance to the reduction profile of a supported cobalt catalyst, than to the reduction profile of bulk Co_3O_4 . The cobalt-alumina interaction decreased the rate of reduction of Co_3O_4 and CoO, which resulted in a shift of the reduction peaks in the TPR to higher temperatures. In conclusion, the position of the Co_3O_4 and CoO peaks in the TPR profile is an indication of the strength of the metal-support interaction, because alumina may block defect sites at the cobalt-alumina interface thus hindering hydrogen activation and nucleation of reduced cobalt phases.

Furthermore, alumina modification led to the appearance of additional reduction peaks at temperatures between 400 and 600 °C, which may be assigned to a cobalt-alumina phase with cobalt in octahedral positions. Reduction peaks at temperatures between 600 and 800 °C were assigned to a cobalt-alumina phase with cobalt in tetrahedral position. Unlike previous reports that suggested the presence of alumina increases the activation energy for cobalt oxide reduction, we conclude that small quantities of alumina mainly have a kinetic effect on the rate of reduction by decreasing the pre-exponential factor.

Acknowledgements This work is based on the research supported by funding from c*change (DST-NRF Centre of Excellence in Catalysis) and in part by the National Research Foundation of South Africa Grant number 94878. The authors wish to gratefully acknowledge the Centre for High Resolution Transmission Electron Microscopy, especially Dr. J. E. Olivier and Dr. J. H. O'Connell, at Nelson Mandela University in Port Elizabeth for their assistance and use of their facilities. This study used resources of the Brazilian Synchrotron Light Laboratory (LNLS), an open national facility operated by the Brazilian Centre for Research in Energy and Materials (CNPEM) for the MCTIC. The XAFS2 beamline staff, especially Dr. S. Figueroa and Dr. A. P. da Silva Sotero Levinsky are acknowledged for the assistance during the experiments.

Compliance with Ethical Standards

Conflict of interest All authors declare no conflict of interest.

References

1. Tauster SJ (1987) *Acc Chem Res* 20:389
2. Fu Q, Wagner T (2007) *Surf Sci Rep* 62:431
3. Jermwongratanaichai T, Jacobs G, Shafer WD, Pendyala VRR, Ma W, Gnanamani MK, Hopps S, Thomas GA, Kitiyanan B, Khalid S, Davis BH (2014) *Catal Today* 228:15
4. Tsakoumis NE, Voronov A, Rønning M, van Beek W, Borg Ø, Rytter E, Holmen A (2012) *J Catal* 291:138
5. Gnanamani MK, Jacobs G, Graham UM, Pendyala VRR, Martinelli M, MacLennan A, Hu Y, Davis BH (2017) *Appl Catal A* 538:190
6. Hilmen AM, Schanke D, Holmen A (1996) *Catal Lett* 38:143
7. Kissinger HE (1957) *Anal Chem* 29:1702
8. Jacobs G, Ji Y, Davis BH, Cronauer D, Kropf AJ, Marshall CL (2007) *Appl Catal A* 333:177
9. Tang CW, Wang CB, Chien SH (2008) *Thermochim Acta* 473:68
10. Sexton BA, Hughes AE, Turney TW (1986) *J Catal* 97:390
11. Rosynek MP, Polansky CA (1991) *Appl Catal* 73:97
12. Ji Y, Zhao Z, Duan A, Jiang G, Liu J (2009) *J Phys Chem C* 113:7186
13. Arnoldy P, Moulijn JA (1985) *J Catal* 93:38
14. Wang WJ, Chen YW (1991) *Appl Catal* 77:223
15. Lapidus A, Krylova A, Kazanskii V, Borovkov V, Zaitsev A, Rathousky J, Zukal A, Jančálková M (1991) *Appl Catal* 73:65
16. Jongsomjit B, Panpranot J, Goodwin JG (2001) *J Catal* 204:98
17. Nabaho D, Niemantsverdriet JW, Claeys M, van Steen E (2016) *Catal Today* 275:27
18. Borg Ø, Eri S, Blekkan EA, Storsæter S, Wigum H, Rytter E, Holmen A (2007) *J Catal* 248:89
19. Kogelbauer A, Goodwin JG Jr, Oukaci R (1996) *J Catal* 160:125
20. van de Loosdrecht J, Barradas S, Caricato EA, Ngwenya NG, Nkwanyana PS, Rawat MAS, Sigwebela BH, van Berge PJ, Visagie JL (2003) *Top Catal* 26:121
21. Bhatia S, Beltramini J, Do DD (1990) *Catal Today* 7:309
22. Ji L, Lin J, Zeng HC (2000) *J Phys Chem B* 104:1783
23. Zhang Y, Wei D, Hammache S, Goodwin JG Jr (1999) *J Catal* 188:281
24. Jacobs G, Das TK, Zhang Y, Li J, Racoillet G, Davis BH (2002) *Appl Catal A* 233:263
25. Chung KS, Massoth FE (1980) *J Catal* 64:320
26. Scherrer P (1918) *Nachr Gesell Wissen Göttingen, Math-Phys Klasse*, 1918:98
27. Langford JI, Wilson AJC (1978) *J Appl Crystallogr* 11:102
28. Ravel B, Newville M (2005) *J Synchrotron Radiat* 12:537
29. Batley GE, Ekstrom A, Johnson DA (1974) *J Catal* 34:368
30. Liu J, Zhang H, Zhou T, Wei S (2000) *Jinshu Xuebao* 36:837
31. Haber J (1977) *J Less Common Metals* 54:243
32. Shulman GR, Yafet Y, Eisenberger P, Blumberg WE (1976) *PNAS* 73:1384
33. Tsakoumis NE, Johnsen RE, Van Beek W, Rønning M, Rytter E, Holmen A (2016) *Chem Commun* 52:3239
34. Kurajica S, Popović J, Tkalčec E, Gržeta B, Mandić V (2012) *Mater Chem Phys* 135:587
35. Chin RL, Hercules DM (1982) *J Phys Chem* 86:360
36. Okamoto Y, Nagata K, Adachi T, Imanaka T, Inamura K, Takyu T (1991) *J Phys Chem* 95:310
37. Bracconi P, Dufour LC (1970) *Cr Acad Sci C Chim* 270:1152

38. Hurst NW, Gentry SJ, Jones A (1982) *Catal Rev* 24:233
39. Burnham AK, Weese RK, Weeks BL (2004) *J Phys Chem B* 108:19432
40. Ward MR, Boyes ED, Gai PL (2014) *J Phys Conf Ser* 522:012009/1
41. Boldyrev VV (1986) *Thermochim Acta* 100:315
42. Johnson GR, Bell AT (2016) *J Catal* 338:250

Affiliations

Anna P. Petersen¹ · Roy P. Forbes² · Sandeeran Govender¹ · Patricia J. Kooyman¹  · Eric van Steen¹ 

¹ Department of Chemical Engineering, Catalysis Institute, University of Cape Town, Private Bag X3, Rondebosch 7701, South Africa

² School of Chemistry, Molecular Sciences Institute, University of the Witwatersrand, Private Bag 3, PO Wits, Johannesburg 2050, South Africa